Temperature dependent crystallization of amorphous $Y_{67}Fe_{33}$ studied using kinetic small angle neutron scattering

2008 J. Phys.: Condens. Matter 20 395230

(http://iopscience.iop.org/0953-8984/20/39/395230)

J. Phys.: Condens. Matter **20** (2008) 395230 (5pp) doi:10.1088/0953-8984/20/39/395230

Temperature dependent crystallization of amorphous $Y_{67}Fe_{33}$ studied using kinetic small angle neutron scattering

M Al-Jawad[1] **and S H Kilcoyne**[2]

[1] Department of Oral Biology, Leeds Dental Institute, University of Leeds, Leeds LS2 9LU, UK
[2] Institute for Materials Research, University of Salford, Salford M5 4WT, UK

E-mail: m.al-jawad@leeds.ac.uk

Received 13 May 2008, in final form 13 August 2008
Published 4 September 2008
Online at stacks.iop.org/JPhysCM/20/395230

Abstract

Temperature-resolved small angle neutron scattering (SANS) has been used to study the nucleation, growth kinetics and crystallite morphology in the Y–Fe system. Crystallization from amorphous $Y_{67}Fe_{33}$ to the YFe_2 Laves phase via a novel 'YFe' intermediate phase has been followed to completion as a function of temperature from 180 to 500 °C. The SANS results agree well with published kinetic neutron diffraction data. Below 390 °C, diffraction data suggest that SANS arises solely from the contrast between crystalline Y and the Fe-rich amorphous matrix. Between 390 and 410 °C all temperature variables are seen to form a sharp peak. This suggests that critical scattering occurs at $T_c \approx 400$ °C. This critical scattering implies that full crystallization of $Y_{67}Fe_{33}$ occurs over a very narrow (∼20 °C) temperature range.

1. Introduction

Studying the kinetics of processes such as crystallization, phase formation and grain growth in metallic systems leads to a deeper understanding of these fundamental physical phenomena, and allows the possibility of tailoring the microstructures of materials for their particular applications. Time-resolved neutron scattering is a particularly powerful technique with which to measure any kinetic process where the neutron scattering lengths of the starting and final materials are sufficiently different to be distinguished. Rare earth–transition metal (RE-TM) alloys are frequently studied because of the interesting magnetic properties they often exhibit [1, 2], and their potential technological applications (high-density permanent magnets, magnetic storage media, and giant magnetoresistive materials). The large number of crystallographic phases, observed in RE-TM systems provide the opportunity to vary magnetic exchange, anisotropy, coercivity, and conduction electron density making them ideal candidates to test theories of magnetic properties of intermetallics, such as the fundamentals of spin fluctuation, moment formation, and magnetic order.

The crystallization processes in rare earth–transition metal binary systems and the associated equilibrium phase diagrams are thought to be well established for most compounds. Phase diagrams are generally constructed using a quenching technique, where samples are heated to the desired temperature and then cooled rapidly. It is assumed that the crystallographic state existing at elevated temperature is 'frozen' into the system. However, this approach has limitations, as was demonstrated by Kilcoyne *et al* in 2001 with the discovery of a new 'YFe' intermediate phase, prepared by carefully annealing amorphous $Y_{67}Fe_{33}$ ribbons whilst monitoring the crystallization processes as a function of time with neutron diffraction [3]. From the results of the study by Kilcoyne *et al*, the crystallization of amorphous $Y_{67}Fe_{33}$ can be fully described. Firstly partial crystallization occurs at 300 °C when elemental Y begins to form. Crystalline Y exists within an iron-rich amorphous matrix, until 390 °C when the whole sample crystallizes. At 390 °C the intermediate 'YFe' phase starts to form, coexisting with elemental Y. This phase only exists over a narrow temperature range (approximately 60 °C). By 450 °C, no Bragg peaks arising from the intermediate 'YFe' phase are observed. Lastly, at 450 °C the YFe_2 Laves phase forms. This phase coexists with pure Y until completion of the reaction at 490 °C.

Observation of the intermediate phase indicated that this was a previously unreported phase which clearly required

Table 1. Refinement parameters from D2B refinement and pattern matching (taken from [3]).

	Phase 1 Y	Phase 2 'YFe'
Space group	$P6_3/mmc$	$P6_3/mmc$
a (Å)	3.628(3)	12.90(1)
c (Å)	5.739(5)	1.171(1)
c/a	1.58	0.91
γ (deg)	120	120
$R_{(\mathrm{Bragg})}$	2.76	1.60

further investigation. Kilcoyne *et al* managed to stabilize the phase at room temperature by rapidly cooling ribbons from 375 °C. Diffraction patterns were collected regularly during cooling, to confirm that the phases present at elevated temperature were unaltered at room temperature [3]. The crystallographic parameters of the 'YFe' intermediate phase were determined using pattern matching analysis with the FullProf program [4] and are given in table 1.

In this paper we present the results of a small angle neutron scattering (SANS) study of nucleation and grain growth during crystallization in the Y–Fe system as a function of temperature. The results are linked to the diffraction data obtained on the D2B diffractometer at ILL, Grenoble and presented in [3].

2. Experimental procedure

Polycrystalline $Y_{67}Fe_{33}$ ingots were produced using an argon arc furnace. High purity elements (99.9% purity Y, and 99.99% purity Fe) were melted together in an argon atmosphere from which any gaseous impurities were removed by first melting a titanium 'getter'. To ensure homogeneity, ingots were melted and turned several times and their masses were limited to 10 g. The ingots were then cut into small pieces (0.7–1.0 g) in preparation for melt spinning. Once melted in a quartz tube, a burst of Ar gas forced the molten sample onto the rapidly rotating copper wheel, cooling it at a rate of $\sim 10^6$ K s^{-1}. Several grams of amorphous ribbon, ~ 20 μm thick and several cm long, were produced using this method.

Approximately 2 g of melt spun $Y_{67}Fe_{33}$ ribbons were mounted in a flat, circular vanadium cell. The sample cell had a radius of 10 mm and a thickness of 2 mm. The cell was mounted in a standard vanadium-element vacuum furnace on the SANS instrument D22 at the Institute Laue Langevin, France. The set up used allowed a Q range of 0.0018–0.015 Å^{-1} to be explored. The ribbons were first heated to 150 °C for 1 h to establish thermal equilibrium, and then heated from 180 to 500 °C (i.e. the temperature range in which all three stages of crystallization can be observed) at 1 °C min^{-1} whilst SANS patterns were collected every minute. In order to compensate the measured intensity to account for the efficiency of the detector and for the detector surface being planar rather than spherical, a standard sample was measured. In our experiment where relative cross-sections, rather than absolute values are required Perspex, which has a uniform cross-section in the Q range of interest, was used as a suitable standard.

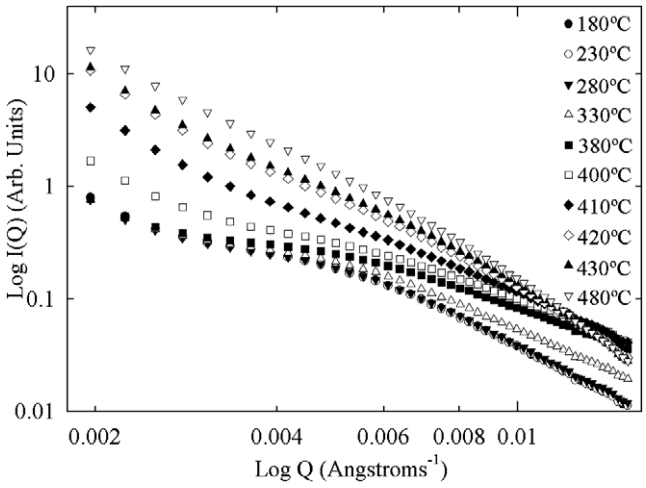

Figure 1. log $I(Q)$ versus log Q at various temperatures during heating at 1 °C min^{-1} of amorphous $Y_{67}Fe_{33}$. Errors lie within the data points. The y-axis has been logarithmically scaled to fit all the curves on the same axes.

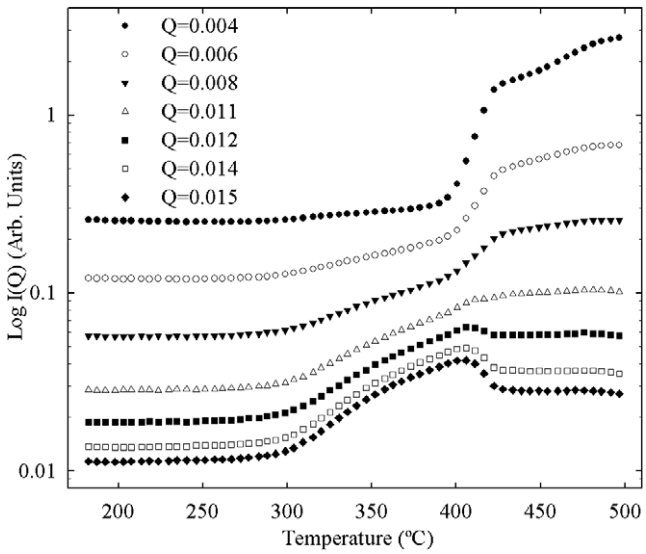

Figure 2. Temperature dependence of the SANS intensity at various values of Q, heating amorphous $Y_{67}Fe_{33}$ at 1 °C min^{-1}. Errors lie within the data points.

3. Results and discussion

Figure 1 shows the variation of $I(Q)$ with Q for several temperatures between 180 and 500 °C plotted on an x–y logarithmic scale. It can be seen from this figure that the Q and temperature dependence of the intensity is not straightforward. In the high Q range, ($Q > 0.01$ Å^{-1}) $I(Q)$ begins to increase at around 330. Between 330 and 380 °C, $I(Q)$ increases in the high Q region, whereas at very low Q, ($Q < 0.004$ Å^{-1}) it remains unchanged. Between 380 and 400 °C $I(Q)$ increases in both the low Q ($Q < 0.006$ Å^{-1}) and high Q regions. Above 400 °C, $I(Q)$ continues to increase at low Q but starts decreasing at high Q.

Figure 2 shows the variation of $I(Q)$ with temperature at several Q values. This plot also illustrates the marked

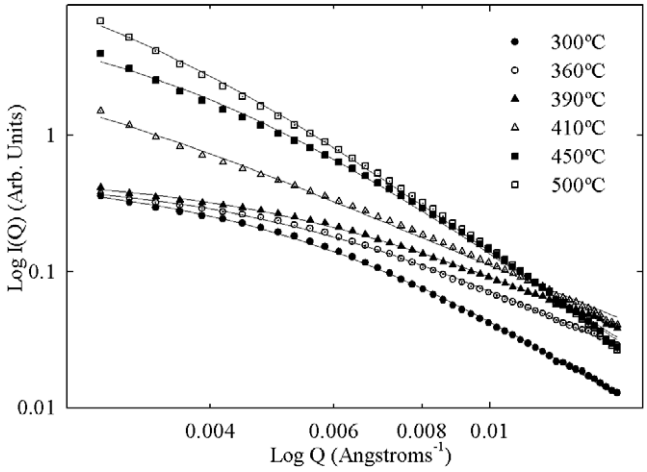

Figure 3. SANS data fitted to the general Lorentzian function given in (1).

difference in the behaviour of $I(Q)$ at low Q and at high Q as a function of temperature. At high Q, $I(Q)$ starts to increase at around 300 °C and continues to increase until ∼410 °C where it peaks. It then decreases between 410 and 430 °C. From 430 to 500 °C $I(Q)$ stays approximately constant in the high Q region. At low Q, $I(Q)$ stays constant until ∼390 °C. From 390 to 420 °C it increases sharply, and from 420 to 500 °C it continues to increase but at a lower rate. At intermediate Q, $0.006\ \text{Å}^{-1} < Q < 0.01\ \text{Å}^{-1}$, the temperature dependence of $I(Q)$ shows behaviour from both the high Q and low Q regimes.

Assuming a monodispersed system of particle sizes, Guinier plots of log $I(Q)$ versus Q^2 for spherical particles were used to estimate the mean particle size [5]. The Guinier approximation is only valid in a limited low Q range up to $QR_G \sim 1.2$ where R_G is the radius of gyration of the spherical particles. In this work, Guinier plots do not give the expected straight line suggesting that a range of particle sizes exists in the Y–Fe system. This is not unexpected since from kinetic neutron diffraction experiments it is known that the crystallization of amorphous $Y_{67}Fe_{33}$ follows a complex multi-stage, multi-phase process. One or more crystalline phases or an amorphous phase coexist at any given temperature and these different phases will have different correlation lengths. Linearity is seen however, in plots of $1/I(Q)$ versus Q^2 and $1/I(Q)^{1/2}$ versus Q^2 which suggests that a Lorentzian or Lorentzian squared distribution would be a more appropriate model for the data. Although strictly only valid in the Guinier region, the generalized Lorentzian function given in equation (1) appears to provide a good description of the data for the entire Q range:

$$I(Q) = \frac{A(\kappa^2)^z}{\left(\kappa^2 + Q^2\right)^z} \tag{1}$$

where A is the scattering amplitude, which is related to the number of particles and the contrast in scattering length density in the material. The range parameter $1/\kappa$, is the average length-scale of fluctuations in scattering length

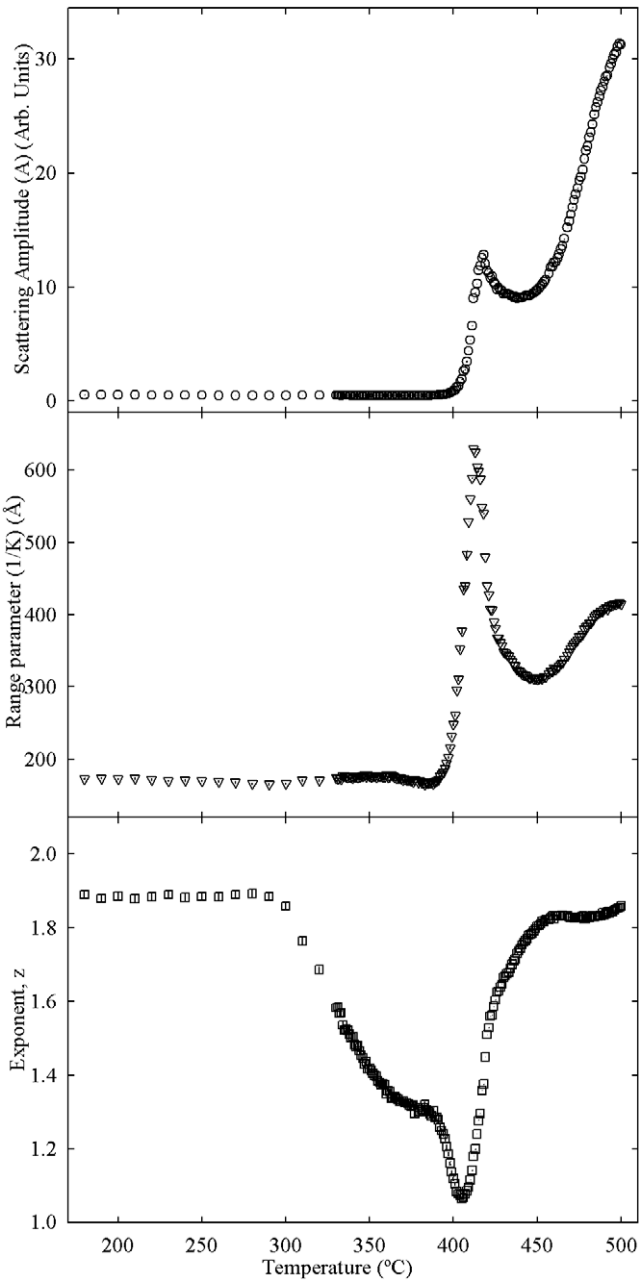

Figure 4. Generalized Lorentzian parameters for fits to SANS data. The errors lie within the data points.

density, and gives the particle size or the distance between particles. z is the power of the Lorentzian term. A power of Lorentzian expression, is observed when scattering arises from a Maxwellian distribution of geometrically similar particles [6]. Equation (1) was used by Boardman *et al* to fit similar structural SANS data collected on D11 (ILL, Grenoble) during the crystallization of amorphous $Bi_2Sr_2CaCu_2O_x$ [7].

Equation (1) fits the SANS data collected during the crystallization of amorphous $Y_{67}Fe_{33}$ extremely well across the whole Q range and temperature range. The fits to the data collected at several temperatures between 300 °C (the start of Y-crystallization) and 500 °C, are shown in figure 3, while figure 4 shows the temperature dependence of the fit parameters A, $1/\kappa$, and z.

It can be seen in figure 4 that for $T < 300\,^{\circ}\mathrm{C}$ the scattering is effectively squared Lorentzian in form ($z \sim 1.9$), indicating that a broad distribution of structural inhomogeneities exist in the melt spun ribbons [8]. The range parameter suggests that these inhomogeneities are ∼170 Å in size. At 300 °C, the power of the Lorentzian term, z, starts decreasing non-linearly reaching ∼1.3 at 390 °C, and then drops rapidly between 390 and 410 °C almost reaching unity at 410 °C. A and $1/\kappa$ do not alter between 300 °C and 390 °C. Between 390 and 410 °C however, while z decreases rapidly, the scattering amplitude A, and the range parameter $1/\kappa$ both increase dramatically. $1/\kappa$ reaches a peak of 700 Å at 410 °C, which is still within the resolution of D22 for our experimental setup. Between 410 and 450 °C z begins to increase and returns to its initial value of ≈1.9 by 450 °C. Over the same temperature range, A decreases to a local minimum and $1/\kappa$ drops rapidly reaching a minimum of 300 Å at 450 °C. Above 450 °C, z remains approximately constant at 1.9 while A and $1/\kappa$ both start to increase again, with $1/\kappa$ reaching a value of 410 Å when the experiment was terminated at 500 °C.

A comparison of temperature dependent SANS data with temperature dependent neutron diffraction data (from Kilcoyne *et al* [3]) during crystallization of amorphous $Y_{67}Fe_{33}$ is given below. Features are seen in both the diffraction data and SANS data at 300 °C, between 390 and 450 °C, and above 450 °C.

At 300 °C

From the diffraction data, it is known that the sample remains amorphous until 300 °C when Y grains start to precipitate out. Using the Scherrer equation on the FWHM of Bragg peaks arising from the Y phase, Kilcoyne *et al* found that Y grains first appear at 300 °C and are 170 Å in size. The same value of 170 Å is found for the range parameter, $1/\kappa$, at the start of heating on D22, which suggests that the $Y_{67}Fe_{33}$ sample used on D22 was not completely amorphous and that Y grains were already present in the ribbons. Unfortunately it was not possible to check the amorphicity of ribbons by diffraction before starting the experiment, however previous studies of $Y_{67}Fe_{33}$ have shown that small quantities of crystalline Y can be present in melt spun ribbons [9]. The value of the power of a Lorentzian parameter, z, was found to be ∼1.9 at 300 °C. Dierker *et al* [8] stated that Lorentzian squared scattering ($z = 2$) can arise from a crystalline phase existing in an amorphous matrix with sharp interfaces between them, agreeing with the argument that nanocrystalline Y grains are present in the amorphous matrix of the melt spun $Y_{67}Fe_{33}$ ribbons.

Between 390 and 450 °C

All three variables in the SANS fits (A, $1/\kappa$ and z) peak between 390 and 410 °C. This suggests that critical scattering occurs in this temperature range and suggests that there is a critical point that defines the transition between one state and another [10]. Ornstein and Zernike demonstrated that during critical scattering, the scattering distribution is Lorentzian in shape [11, 12]. In addition, Birgeneau *et al* [13] showed that the Fourier transform of the correlation function $C(Q)$ could be written as:

$$C(Q) \propto \frac{\kappa^{p}}{\left(\kappa^{2} + Q^{2}\right)} \tag{2}$$

where p is the critical exponent and $1/\kappa$ is the correlation length (or range parameter). For the case of $z = 1$, equations (1), and (2) are equivalent with a critical exponent of $p = 2$.

Generally, there are two possible causes for the critical scattering seen in structural SANS data. The first is that a percolation threshold has been reached at a critical temperature, T_c. The second is that critical scattering is occurring near T_c in a continuous, higher order phase transition. The neutron diffraction data collected by Kilcoyne *et al* [3] show that at ∼390 °C there is a large drop in the background signal as the whole sample crystallizes. It is clear from this that the $Y_{67}Fe_{33}$ sample fully crystallizes extremely rapidly at ∼390 °C whilst at the same temperature the new 'YFe' phase appears. This points to the critical scattering seen in the SANS data being caused by the sudden crystallization of the whole sample—i.e. a percolation threshold. The rapid increase in $1/\kappa$ as the temperature approaches T_c therefore suggests that there is an increase in the average grain size as the crystallites grow and impinge on one another prior to the effectively infinite crystalline cluster being formed at the percolation threshold. A value of $T_c \approx 400\,^{\circ}\mathrm{C}$ can be extracted for the critical temperature of the full crystallization of amorphous $Y_{67}Fe_{33}$.

Above 450 °C

From diffraction data, 450 °C is the temperature at which the new 'YFe' phase transforms into YFe_2. Also above 450 °C is when the Y grains grow most rapidly. SANS above T_c at $T >$ 450 °C can therefore be explained by the phase transformation from the new 'YFe' phase to YFe_2 as the atoms reorder and the Y and YFe_2 grains grow.

4. Conclusions

Small angle neutron scattering has been used to study the temperature dependent crystallization of amorphous $Y_{67}Fe_{33}$. The results can be described extremely well by a general Lorentzian function, and the data are in good agreement with the neutron diffraction study by Kilcoyne *et al*. At low temperatures, diffraction data suggest that SANS arises solely from the contrast between crystalline Y and the Fe-rich amorphous matrix. At $T \sim 400\,^{\circ}\mathrm{C}$ critical scattering is observed corresponding to the full crystallization of the sample. Above 410 °C, trends in A, $1/\kappa$ and z can be followed as a function of temperature, but having a complex multi-phase system makes it is difficult to isolate the individual range parameters, $1/\kappa$, for each crystallographic phase (Y, 'YFe' or YFe_2).

Until now the lowest reported Fe concentration in a Y–Fe compound was ∼67%, (YFe_2) but, through the formation of this phase, this has now been reduced to 50%. It is hoped that it will be possible to isolate this phase, and through understanding how the magnetic properties relate to

the crystallographic properties and growth morphologies we will be able to tailor micro- and nano-structured materials with interesting technological applications.

Acknowledgments

The authors would like to thank Dr Ross Stewart at the Institute Laue Langevin for his assistance during the small angle neutron scattering experiment and for help with data processing and normalization. In addition we thank Professor Bob Cywinski for his guidance and useful discussions.

References

[1] Wallace W E 1973 *Rare Earth Intermetallics* (New York: Academic)
[2] Franse J J M and de Boer F R 1995 *J. Magn. Magn. Mater.* **140** 789–92
[3] Kilcoyne S H, Manuel P and Ritter C 2001 *J. Phys.: Condens. Matter* **13** 5241–50
[4] Rodriguez-Carvajal J 1990 FULLPROF: a program for Rietveld refinement and pattern matching analysis *Satellite Mtg on Powder Diffraction of the XV Congr. of the IUCr (Toulouse)* p 127 (Abstracts)
[5] Guinier A 1963 *X-Ray Diffraction in Crystals, Imperfect Crystals and Amorphous Bodies* (London: Freeman)
[6] Guinier A and Fournet G 1955 *Small Angle Scattering of X-rays* (New York: Wiley)
[7] Boardman C J, Kilcoyne S H and Cywinski R 1991 *Physica* C **185** 633–4
[8] Dierker S B and Wiltzius P 1991 *Phys. Rev. Lett.* **66** 1185–8
[9] Al-Jawad M 2004 Time-resolved neutron studies of metallic phase formation *PhD Thesis* University of Leeds
[10] Gerold V and Kostorz G 1978 *J. Appl. Crystallogr.* **11** 376–404
[11] Ornstein L S and Zernike F 1914 *Proc. Amst. Akad. Sci.* **17** 793–806
Zernicke F 1916 *Proc. Amst. Akad. Sci.* **18** 1520–7
Ornstein L S and Zernike F 1917 *Proc. Amst. Akad. Sci.* **19** 1312–5
[12] Ornstein L S and Zernike F 1918 *Phys. Z.* **19** 134–7
Ornstein L S and Zernike F 1926 *Phys. Z.* **27** 761–3
[13] Birgeneau R J, Cowley R A, Shirnae G, Tarvin J A and Guggenheim H J 1980 *Phys. Rev.* B **21** 317–32